Journal of Alloys and Compounds 515 (2012) 22–25

Contents lists available at SciVerse ScienceDirect

Journal of Alloys and Compounds

journal homepage: www.elsevier.com/locate/jallcom

Letter

Phase structure and microwave dielectric properties of $(1-x)Li_2Zn_3Ti_4O_{12}-xTiO_2$ ceramics

Xiaobin Liu, Huanfu Zhou*, Xiuli Chen, Liang Fang

State Key Laboratory Breeding Base of Nonferrous Metals and Specific Materials Processing, Key Laboratory of Nonferrous Materials and New Processing Technology, Ministry of Education, Guilin University of Technology, Guilin 541004, China

ARTICLE INFO

Article history:
Received 14 October 2011
Received in revised form
23 November 2011
Accepted 25 November 2011
Available online 2 December 2011

Keywords:
Microwave dielectric properties
X-ray diffraction
Sintering
Cubic structure

ABSTRACT

Microwave dielectric ceramics with the composition of $(1-x)Li_2Zn_3Ti_4O_{12}$ (LZT)–$xTiO_2$ ($0 \le x < 1$) were prepared by the solid-state reaction method. The crystal structures were determined by X-ray diffraction. $(1-x)$LZT–$xTiO_2$ solid solutions show a cubic structure [$P4_332$ (2 1 2)] similar to $Zn_2Ti_3O_8$ in the range of $0.2 \le x \le 0.4$. When the x value reaches 0.6, the rutile TiO_2 phase appears. The microwave dielectric properties were studied by a Network Analyzer. The relative permittivity (ε_r) and temperature coefficients of resonant frequency (τ_f) were adjusted with increasing x values. Especially, 0.4LZT–0.6TiO_2 ceramic exhibits good microwave dielectric properties with a ε_r of 25.1, a high $Q \times f$ of 62,000 GHz and a near-zero τ_f of −5.2 ppm/°C.

1. Introduction

The recent progress in microwave telecommunication, satellite broadcasting and intelligent transport systems (ITS) has resulted in an increasing demand for dielectric resonators (DRs). Dielectric resonators generally consist of a puck of ceramic that has high permittivity and low dissipation factor. The resonant frequency of a DR is determined by the overall physical dimensions of the puck, the permittivity of the material and its immediate surroundings. The key properties are high-quality factor (Q), high relative permittivity (ε_r) and near-zero temperature coefficient of resonant frequency (τ_f). However, an optimal DR that satisfies these three properties simultaneously is difficult to achieve in a particular material [1–3].

Recently, a number of microwave dielectric ceramics have been developed, such as $Ca(B'_{1/2}Nb_{1/2})O_3$ [B′ = La, Pr, Nd, Sm, Eu, Gd, Tb, Y, Er, Yb and In] [4] and MAl_2O_4 (M = Zn and Mg) [5–7]. However, most of these ceramics have a large negative τ_f value. Generally, there are two methods to design a material with a stable temperature coefficient: (1) composite materials by mixing component materials [8] with negative and positive τ_f values, such as $Zn_2Te_3O_8$–TiO_2 [9], Zn_2TiO_4–TiO_2 [10], $Ca_2P_2O_7$–TiO_2 [11], $CaWO_4$–TiO_2 [12], $Mg_4Ta_2O_9$–TiO_2 [13] and $LiNb_3O_8$–TiO_2 [14]. (2) Formation of solid solutions, such as complex perovskites [15] and other systems [16–17]. More recently, Wu et al. [18] reported temperature stable microwave dielectric ceramic $0.3Li_2TiO_3$–$0.7Li(Zn_{0.5}Ti_{1.5})O_4$ with ultra-low dielectric loss by composite method. In our recent investigation, $ZnLi_{2/3}Ti_{4/3}O_4$ ceramic presents excellent microwave dielectric properties with $\varepsilon_r = 20.6$, $Q \times f = 106{,}700$ GHz, $\tau_f = -48$ ppm/°C[19]. In order to enhance the ε_r and τ_f values, rutile TiO_2 ($\varepsilon_r = 105$, $Q \times f = 46{,}000$ GHz, $\tau_f = +465$ ppm/°C) [20] was added to the LZT ceramic. In this work, sintering characteristics, phase structure and microwave dielectric properties of $(1-x)$LZT–$xTiO_2$ ceramics have been investigated.

2. Experimental

In order to synthesize LZT powders, high-purity powders of Li_2CO_3 (≥99%, Guo-Yao Co. Ltd., Shanghai, China), ZnO (≥99%, Guo-Yao Co. Ltd., Shanghai, China) and TiO_2 (≥99%, Guo-Yao Co. Ltd., Shanghai, China) were weighed according to the molar ratio of 1:3:4. The mixture was ball-milled in a polyethylene bottle with ZrO_2 media for 4 h using alcohol as a medium. The wet mixture was rapidly dried and then calcined at 950 °C for 6 h. Afterward, mixtures of the $(1-x)$LZT–$xTiO_2$ powders (x = 0.2, 0.4, 0.6 and 0.8) were ball-milled in a polyethylene bottle with ZrO_2 media for 4 h using alcohol as a medium. The milled powders were dried, granulated and pressed into cylinders of 12 mm in diameter and 6–8 mm in height by uniaxial pressing under a pressure of 200 MPa. The samples were heated at 550 °C for 4 h to remove the organic binder and then sintered at 1050–1175 °C for 4 h at a heating rate of 5 °C/min.

The bulk density of the sintered samples was measured by Archimedes method. The phase structure of samples was investigated by using X-ray diffractometer (XRD) (Cu$K\alpha_1$, 1.54059 Å, Model X'Pert PRO, PANalytical, Almelo, Holland). The surface micrographs of the samples were examined by using a scanning electron microscope (SEM, Model JSM6380-LV, JEOL, Tokyo, Japan).

Dielectric behaviors in microwave frequency were measured by the $TE_{01\delta}$ shielded cavity method using a Network Analyzer (Model N5230A, Agilent Co., Palo Alto, CA) and a temperature chamber (Delta 9039, Delta Design, San Diego, CA).

* Corresponding author. Tel.: +86 773 5896435.
E-mail address: zhouhuanfu@163.com (H. Zhou).

0925-8388/$ – see front matter © 2011 Elsevier B.V. All rights reserved.
doi:10.1016/j.jallcom.2011.11.116

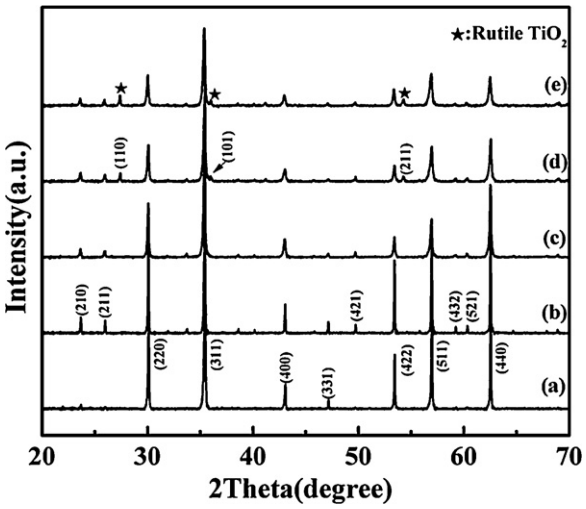

Fig. 1. XRD profiles for the $(1-x)$LZT–xTiO$_2$ ceramics sintered at 1075 °C for 4 h: (a) $x = 0$, (b) $x = 0.2$, (c) $x = 0.4$, (d) $x = 0.6$ and (e) $x = 0.8$.

The temperature coefficients of resonant frequency τ_f values were calculated by the formula as in the following:

$$\tau_f = \frac{f_T - f_0}{f_0(T - T_0)} \quad (1)$$

where f_T, f_0 were the resonant frequencies at the measuring temperature T (85 °C) and T_0 (25 °C), respectively.

3. Results and discussion

Fig. 1 shows the X-ray diffraction (XRD) profiles of the $(1-x)$LZT–xTiO$_2$ ($x = 0$, 0.2, 0.4, 0.6 and 0.8) samples sintered at 1075 °C for 4 h. Pure LZT has a cubic structure [*Fd*-3*m* (2 2 7)] similar to $MgFe_2O_4$ with lattice parameters of $a = 8.401(7)$ Å, $V = 593.07$ Å^3, $\rho = 4.43$ g/cm^3 and $Z = 8$ (Z denotes the number of unit cell molecules in a unit cell) [19]. However, as x value is over 0.2, the added reflection peaks with (2 1 0), (2 1 1), (4 2 1), (4 3 2) and (5 2 1) show lower symmetry of crystal structure. $(1-x)$LZT–xTiO$_2$ solid solution ($0.2 \le x \le 0.4$) has a cubic structure [$P4_332$ (2 1 2)] similar to $Zn_2Ti_3O_8$ (JCPDS #087-1781). At the region of $x \ge 0.6$, rutile TiO$_2$ phase (JCPDS #071-0650) was observed, and the amount of rutile TiO$_2$ phase increases with increasing the x values. The phase composition, crystallographic parameters of $(1-x)$LZT–xTiO$_2$ ($0 \le x < 1$) ceramics sintered at 1075 °C are shown in Table 1. The structure changes from [*Fd*-3*m* (2 2 7)] to [$P4_332$ (2 1 2)], and the lattice constant decreased from 8.401(7) Å to 8.393(6) Å. However, the calculated density increased from 4.43 g/cm^3 (at $x = 0$) to 4.84 g/cm^3 (at $x = 0.4$), which was attributed to the trace change in cell volume and the increase of molar mass caused by that Ti^{4+} in titanium dioxide entered the unit cell. At the region of $x \ge 0.6$, rutile TiO$_2$ phase was observed, and the mass percentage of the rutile TiO$_2$ phase increased from 12.5% (at $x = 0.6$) to 30.6% (at $x = 0.8$) (calculated via the RIR method in the jade 6.0 software).

The microstructure of the $(1-x)$LZT–xTiO$_2$ ceramics was observed using scanning electron microscopy (SEM). Fig. 2 illustrates SEM images of the $(1-x)$LZT–xTiO$_2$ ceramics sintered at 1075 °C. The well-densified microstructures were obtained and little porosity was observed in the sintered samples. The pure LZT ceramic [Fig. 2(a)] has a dense microstructure with the average grain size of ~50 μm. The grain size becomes smaller with increasing TiO$_2$ contents, which may be contributed by its high sintering temperature (above 1300 °C). In particular, a small amount of tetragonal rutile TiO$_2$ were firstly observed in Fig. 2(d) (at $x = 0.6$), which agree well with the analysis of X-ray diffraction patterns. As the x value is 0.8, the rod-like TiO$_2$ grains with a width size of about 2 μm and square grains with a size of about more than 5 μm were observed [as shown in Fig. 2(e)].

The bulk density, $Q \times f$ values and relative permittivity of the $(1-x)$LZT–xTiO$_2$ samples as a function of the sintering temperatures are shown in Fig. 3. The bulk densities initially increase with increasing x values from 0.2 to 0.6 and then slightly decrease with further increasing the x values. The increase of the bulk densities can be explained by the produce of phase with higher crystallographic calculated density (as shown in Table 1). In addition, the decrease of the densities may be the emergence of excessive TiO$_2$ with relatively lower density (4.25 g/cm^3) as well as the reduction of the sintering characteristics of the LZT ceramics due to the high sintering temperature of TiO$_2$ (above 1300 °C). It is noticeable that the $(1-x)$LZT–xTiO$_2$ ceramics have a relatively wide sintering temperature range (above 100 °C), which can be illustrated by the trace change in densities for the whole sintering temperatures. The relative permittivity increases with increasing x values. The effect of sintering temperature on the permittivity is not obvious for the same composition, which is consistent with the little change of the bulk density of the $(1-x)$LZT–xTiO$_2$ ceramics for the same x value at different temperatures. The $Q \times f$ values decreased with increasing x values when the sintering temperatures are lower than 1075 °C. However, the $Q \times f$ values initially decreased between $x = 0.2$ and 0.6 and then increased between $x = 0.6$ and 0.8 when the sintering temperatures are higher than 1100 °C. At the region of $0.4 \le x \le 0.6$, the decrease of the $Q \times f$ values at different sintering temperature was resulted from the produce of the TiO$_2$ phase. Overall, the optimal sintering temperature of the $(1-x)$LZT–xTiO$_2$ ceramics ($x \le 0.6$) is 1075 °C.

Fig. 4 shows the temperature coefficients of resonant frequency τ_f of the $(1-x)$LZT–xTiO$_2$ ceramics sintered at 1075 °C, insert shows the τ_f values of the 0.4LZT–0.6TiO$_2$ ceramics as a function of the sintering temperatures. The τ_f values increase slightly in the x range of $0.2 \le x \le 0.4$, which may be attributed to the trace change in the crystal structure. However, due to the secondary phase TiO$_2$, the τ_f values shift sharply in the range of $0.4 < x \le 0.8$. Especially, when x value reach to 0.6, the τ_f values is near to zero, which is attributed to appropriate amount of TiO$_2$ with very high τ_f value (~+465 ppm/°C) [20]. The τ_f values of the 0.4LZT–0.6TiO$_2$ ceramics at different sintering temperatures have no obvious change and keep relatively steady. Hence, the 0.4LZT–0.6TiO$_2$ ceramics sintered at 1075 °C have excellent microwave dielectric properties with a ε_r of 25.1, a high $Q \times f$ of 62,000 GHz and a τ_f of −5.2 ppm/°C.

Table 1
Phase composition and crystallographic parameters of $(1-x)$LZT–xTiO$_2$ ceramics sintered at 1075 °C.

x values	Phase composition	Secondary phase wt (%)	Crystallographic parameters		
			Lattice constant, a (Å)	Volume of cell, V (Å^3)	Calculated density, ρ (g/cm^3)
$x = 0$	Single	–	8.401(7)	593.07	4.43
$x = 0.2$	Single	–	8.393(6)	591.35	4.59
$x = 0.4$	Single	–	8.395(8)	591.82	4.84
$x = 0.6$	Mixture	TiO$_2$: 12.5%	–	–	–
$x = 0.8$	Mixture	TiO$_2$: 30.6%	–	–	–

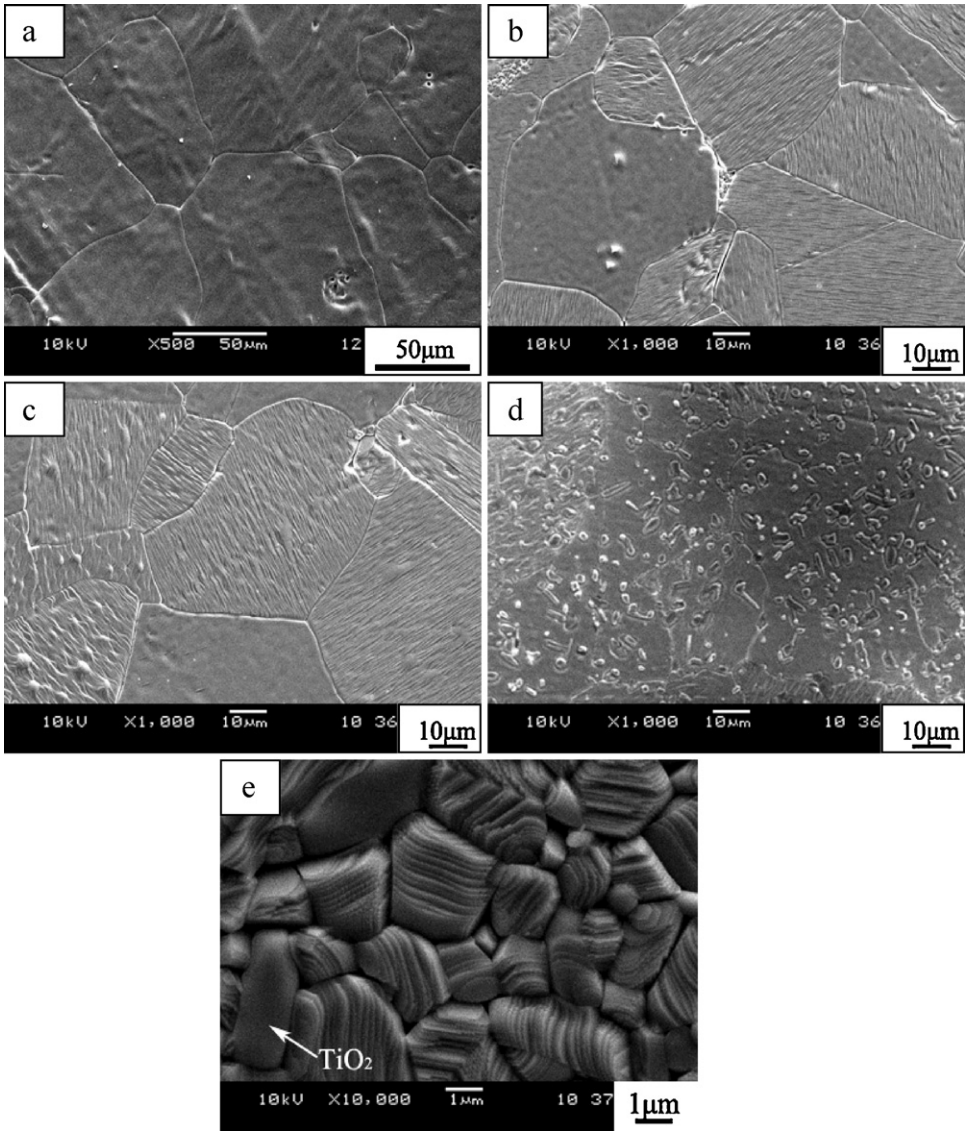

Fig. 2. The SEM micrographs of the $(1-x)$LZT–xTiO$_2$ ceramics sintered at 1075 °C: (a) $x = 0$, (b) $x = 0.2$, (c) $x = 0.4$, (d) $x = 0.6$ and (e) $x = 0.8$.

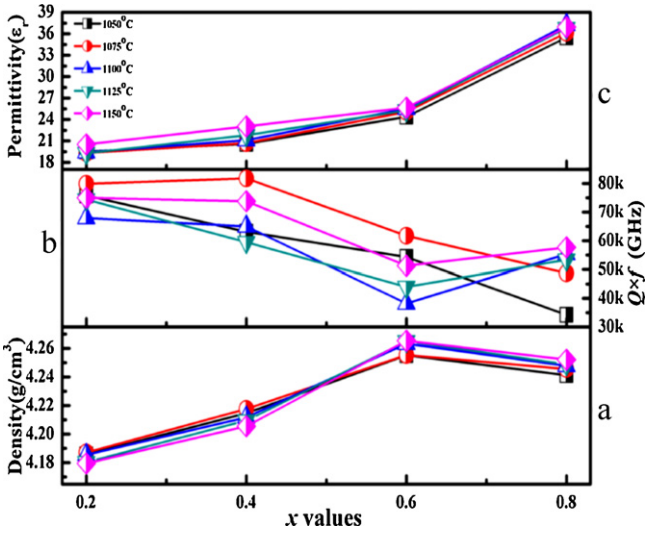

Fig. 3. The bulk density (a), $Q \times f$ (b) and relative permittivity (c) of $(1-x)$LZT–xTiO$_2$ ceramics as a function of the sintering temperature.

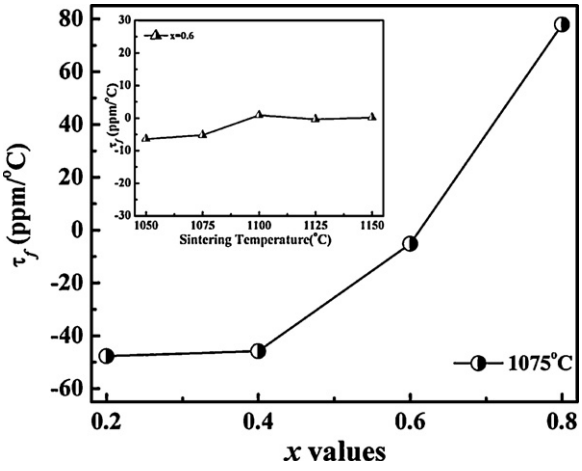

Fig. 4. The τ_f values of $(1-x)$LZT–xTiO$_2$ ceramics sintered at 1075 °C as a function of the TiO$_2$ content. The inset shows τ_f values of the 0.4LZT–0.6TiO$_2$ ceramics as a function of the sintering temperatures.

4. Conclusion

In this study, the structure and microwave dielectric properties of the $(1-x)$LZT–$x$$TiO_2$ ceramics were investigated. $(1-x)$LZT–$x$$TiO_2$ ($x \geq 0.2$) has a cubic structure [$P4_332$ (2 1 2)] similar to $Zn_2Ti_3O_8$, the rutile TiO_2 phase appeared as x values are over 0.6. $(1-x)$LZT–$x$$TiO_2$ ceramics exhibited good dielectric properties. Especially, 0.4LZT–0.6TiO_2 ceramic has excellent microwave dielectric properties with a ε_r of 25.1, a high $Q \times f$ of 62,000 GHz and a near-zero τ_f of -5.2 ppm/°C.

Acknowledgements

This work was supported by Natural Science Foundation of China (No. 51102058, No. 50962004 and No. 21061004), Natural Science Foundation of Guangxi (No. 2011GXNSFB018012 and No. 2011GXNSFB018009), Research start-up funds Doctor of Guilin University of Technology (No. 002401003281 and No. 002401003282), and Program for NCET-06-0656, MOE, China.

References

[1] T. Sebastian, Dielectric Materials for Wireless Communications, Elseiver Publishers, Oxford, UK, 2008.
[2] L. Fang, D.J. Chu, H.F. Zhou, X.L. Chen, H. Zhang, B.C. Chang, C.C. Li, Y.D. Qin, X. Huang, J. Alloys Compd. 35 (2011) 8840–8844.
[3] X.L. Chen, H.F. Zhou, L. Fang, X.B. Liu, Y.L. Wang, J. Alloys Compd. 19 (2011) 5829–5832.
[4] L.A. Khalam, M.T. Sebastian, J. Am. Ceram. Soc. 90 (2007) 1467–1474.
[5] K.P. Surendran, N. Santha, P. Mohanan, M.T. Sebastian, Eur. Phys. J. B 41 (2004) 301–306.
[6] K.P. Surendran, P.V. Bijumon, P. Mohanan, M.T. Sebastian, Appl. Phys. A 81 (2005) 823–826.
[7] W. Lei, W.-Z. Lu, J.-H. Zhu, X.-H. Wang, Mater. Lett. 61 (2007) 4066–4069.
[8] J. Guo, D. Zhou, H. Wang, X. Yao, J. Alloys Compd. 509 (2011) 5863–5865.
[9] G. Subodh, M.T. Sebastian, J. Am. Ceram. Soc. 90 (2007) 2266–2268.
[10] C.F. Shih, W.M. Li, M.M. Lin, C.Y. Hsiao, K.T. Hung, J. Alloys Compd. 485 (2009) 408–412.
[11] I.S. Cho, S.K. Kang, D.W. Kim, K.S. Hong, J. Eur. Ceram. Soc. 26 (2006) 2007–2010.
[12] S.H. Yoon, G.K. Choi, D.W. Kim, S.Y. Cho, K.S. Hong, J. Eur. Ceram. Soc. 27 (2007) 3087–3091.
[13] J.S. Kim, E.S. Choi, K.W. Ryu, S.G. Bae, Y.H. Lee, Mater. Sci. Eng. B 162 (2009) 87–91.
[14] S.O. Yoon, J.H. Yoon, K.S. Kim, S.H. Shim, Y.K. Pyeon, J. Eur. Ceram. Soc. 26 (2006) 2031–2034.
[15] Z. Liang, L.L. Yuan, J.J. Bian, J. Alloys Compd. 509 (2011) 1893–1896.
[16] D. Zhou, W.G. Qu, C.A. Randall, L.X. Pang, H. Wang, X.G. Wu, J. Guo, G.Q. Zhang, L. Shui, Q.P. Wang, H.C. Liu, X. Yao, Acta Mater. 59 (2011) 1502–1509.
[17] D. Zhou, H. Wang, Q.P. Wang, J. Guo, G.Q. Zhang, L. Shui, X. Yao, C.A. Randall, L.X. Pang, H.C. Liu, Funct. Mater. Lett. 3 (2010) 253–257.
[18] Y. Wu, D. Zhou, J. Guo, L.X. Pang, H. Wang, X. Yao, Mater. Lett. 65 (2011) 2680–2682.
[19] H.F. Zhou, X.B. Liu, X.L. Chen, L. Fang, Y.L. Wang, J. Eur. Ceram. Soc. 32 (2012) 261–265.
[20] K. Fukuda, R. Kitoh, I. Awai, Jpn. J. Appl. Phys. 32 (1993) 4584–4588.